



# The Impact of Drop Test Conditions on Brain Strain Location and Severity: A Novel Approach Using a Deep Learning Model

George Stilwell<sup>1</sup> · Danyon Stitt<sup>1</sup> · Keith Alexander<sup>1</sup> · Nick Draper<sup>2</sup> · Natalia Kabaliuk<sup>1</sup>

Received: 16 January 2024 / Accepted: 23 April 2024  
© The Author(s) 2024

## Abstract

In contact sports such as rugby, players are at risk of sustaining traumatic brain injuries (TBI) due to high-intensity head impacts that generate high linear and rotational accelerations of the head. Previous studies have established a clear link between high-intensity head impacts and brain strains that result in concussions. This study presents a novel approach to investigating the effect of a range of laboratory controlled drop test parameters on regional peak and mean maximum principal strain (MPS) predictions within the brain using a trained convolutional neural network (CNN). The CNN is publicly available at <https://github.com/Jilab-biomechanics/CNN-brain-strains>. The results of this study corroborate previous findings that impacts to the side of the head result in significantly higher regional MPS than forehead impacts. Forehead impacts tend to result in the lowest region-averaged MPS values for impacts where the surface angle was at 0° and 45°, while side impacts tend to result in higher regional peak and mean MPS. The absence of a neck in drop tests resulted in lower regional peak and mean MPS values. The results indicated that the relationship between drop test parameters and resulting regional peak and mean MPS predictions is complex. The study's findings offer valuable insights into how deep learning models can be used to provide more detailed insights into how drop test conditions impact regional MPS. The novel approach used in this paper to predict brain strains can be applied in the development of better methods to reduce the brain strain resulting from head accelerations such as protective sports headgear.

**Keywords** Concussion · Brain strain · Rugby · Rotational motion · Finite element

## Introduction

Traumatic brain injuries (TBI) are a significant public health issue, resulting from a bump, blow, or jolt to the head or a penetrating head injury. In the United States alone, TBI causes approximately 2.2 million emergency department visits annually [1, 2]. Several studies have recognised the connection between high-intensity head impacts and

concussions [3–6]. Rugby players, for example, are exposed to an average of 14–52 head impacts per game, with a peak linear acceleration above 10 g [7–10]. Unsurprisingly, mild traumatic brain injuries (mTBI), commonly labelled as concussions, are one of the most frequent injuries sustained by rugby players [11–13]. Prolonged exposure to high-intensity head acceleration events have been linked to a number of long-term mood and cognitive deficits including neurodegenerative diseases such as chronic traumatic encephalopathy and early onset Alzheimer's [14–20]. The reported incidence rates of concussion vary dramatically due to the ill-defined nature of what constitutes a “concussion” [21], with under-reporting rates of concussion estimated to be as high as 50–90% in contact sports such as rugby league [22, 23]. As a result, sport-related concussions have been described as a “silent epidemic” [24].

Attempts to quantify the risk of a given head impact resulting in an mTBI have led to the development of several brain injury criteria (BIC) [4–6, 25, 26]. The head injury criterion (HIC) and rotational injury criterion (RIC) are

---

Associate Editor Stefan M. Duma oversaw the review of this article.

---

George Stilwell and Danyon Stitt have contributed equally to this work.

---

✉ Natalia Kabaliuk  
natalia.kabaliuk@canterbury.ac.nz

<sup>1</sup> Department of Mechanical Engineering, University of Canterbury, Christchurch 8041, New Zealand

<sup>2</sup> Faculty of Health, University of Canterbury, Christchurch 8041, New Zealand

well-known examples of metrics that have been developed using time series kinematic measures of the head during the impact. The use of single variable metrics such as peak linear acceleration (PLA) and BIC alone, however, does not provide a detailed region-specific mechanical response of the brain [27]. Zhan et al. have shown the accuracy of a given BIC metric decreases when applied to a head impact context outside that in which it was developed [15]. Typically, BIC measures are too oversimplified to provide adequate detail of tissue-level insights of TBIs [28]. As a result, there is no consensus between researchers on an appropriate kinematics-based injury metric or a tolerance threshold for sports-related concussion [29]. It should be noted, however, that rotational motion has long been implicated as a primary driver of mTBI symptoms [30–32].

Many studies have shown brain strain, particularly maximum principal strain (MPS), to be a primary mechanism and thus an effective predictor of TBI [25, 31, 33, 34]. The development of dozens of finite element models have enabled researchers a more detailed method to analyse the mechanical response of the brain during an impact [35–38]. One study investigated the effect of impact location on the concussion risk of American football players using two FE models to evaluate the magnitude and distribution of regional brain strains [39]. Laboratory impact tests were used to gather kinematic data using two impact speeds and 12 impact directions. Results from the Simulated Injury Monitor (SIMon) and Global Human Body Model Consortium (GHBMC) models suggested that frontal impacts to the crown and forehead resulted in the lowest brain strain values [39]. Similarly, a study completed using kinematic data from head impact youth football players found that impacts to the top of the helmet were associated with lower strain metrics [40]. Impacts to the side of the helmet were associated with the highest peak rotational velocity and strain metrics [40]. These results corroborate with a study that compared the brain response of frontal and lateral impacts using FE modelling, with predicted shear stress in the brain being much higher in lateral impacts [41].

Due to the complexity of these models, simulations are resource intensive, with some requiring hours of computation time [42–44]. As a consequence, this has limited the routine use of models in practical applications, such as immediate TBI assessment of sports players following an on-field head impact [45]. Until recently, kinematic data from on-field impacts were only analysed days or weeks after the event [46]. Methods to reduce computation time often simultaneously reduce the accuracy of the model outputs, especially for large strain impacts [33, 47]. In contrast, the pre-computation technique put forward by Ji et al. has enabled element-wise, whole-brain MPS to be computed instantly [27]. Once trained on a large library of head impacts, machine learning head models (MLHMs) have

enabled whole-brain MPS to be computed in seconds [48, 49]. Recently, a convolutional neural network (CNN) has been developed and trained using simulation results of head impacts using the Worcester Head Injury Model (WHIM) [50, 51]. The pre-trained CNN enables the nonlinear impact strain relationship to be computed in milliseconds based on the rotational velocity profile of the head [52]. Following the development of these initial MLHMs, a range of research groups have developed subsequent models for a range of applications such as the evaluation of protective helmets and the simulation of head impacts in situations including sports and traffic accidents [53–55]. Such models are capable of acting as a rapid estimation FE model and could accelerate the understanding of mTBI during future studies. Although MLHMs are able to rapidly estimate brain strains, the accuracy of these types of models has been shown to be dependent on the situation in which they are applied in relation to the head impact training data that were used to develop the model [56, 57]. Model accuracy has been shown to decrease when the training datasets are from a range of different impact types such as car accidents, boxing, and college football [56, 57]. Therefore, care needs to be taken when interpreting the results from these models, especially when the head impact training data of the model differ from the application when the model is being employed.

Previous work investigating the effect of drop test condition on the shape of the kinematic profiles of a Hybrid III (HIII) headform found rotational velocity to be largely unaffected [58]. This study aimed to deepen this analysis by investigating the relationship between drop test condition on the location and severity of MPS within the brain. The results of this study could be applied to better understand the relation between field and lab head impact conditions and may act to better understand the biomechanics behind injurious gameplay.

## Materials and Methods

### Experimental Procedure

All impacts were carried out on a twin wire guided drop test rig using a HIII headform (50th percentile male model) instrumented with a nine accelerometer package (NAP) [59]. Three variations of the drop test method were carried out for comparison based on previous work by Stitt et al. and Draper et al. The first used a HIII head and a standard 1-inch Modular Elastomer Pad (MEP) for the impact surface (manufactured by Cadex Inc.), with no neck involved [58, 60]. The second and third drop test variations used were taken from the same authors' study of rugby headgear [61]. Using the same HIII head and neck, and standard 1-inch MEP pad impact surface, drop tests were

carried out with the impact surface angled at  $0^\circ$  and  $45^\circ$  relative to the test rig base. For all tests, the MEP pad was securely bolted to the base of the drop tower. The MEP pad did not slip or separate from the impact surface during laboratory testing. All three drop test variations were carried out across 4 impact locations: forehead (sagittal rotation), front boss, side (coronal rotation), and rear boss (labelled rear-rear boss), as shown in Figure 1. The front boss and rear boss impacts induce multi-axial rotations. Impacts onto the  $45^\circ$  impact surface also included a fifth impact location labelled side-rear boss. All impacts were completed in the orientations shown in Figure 1. With the exception of the rear-rear boss impact for the  $45^\circ$  impacts, all impacts were on the right side of the head. Care should be taken when comparing the resulting strain predictions to the left and right side of the cerebrum for this impact condition compared to the others used in the study. The combination of each impact location and impact surface angle will be hereon referred to as different impact *conditions*. Each impact condition was repeated 5 times at each drop height, with 60 seconds between each repeat.

Unlike the cited studies, trends between drop heights were assumed to be adequately captured by two drop heights. For this reason, only drop heights of 150 and 450 mm were used in this study. Impacts onto the  $45^\circ$  impact surface were assumed to create motions that were only allowable by a flexible neck. The occipital condyle joint on the HIII head does not permit such movement; therefore,  $45^\circ$  impacts without the neck were excluded from the study. A summary of the drop test conditions is outlined in Table 1. To determine the impact energy, the mass of the head and neck of 5.6 kg and the total falling mass of 6.8 kg (including the drop frame) were used.

## Data Acquisition and Post Processing

The HIII headform was instrumented with four triaxial accelerometers (Analog Devices ADXL377, 20,000 Hz, range:  $\pm 200$  g, sensitivity: 6.5 mV/g) creating a NAP with three redundant sensing axes. This allowed linear and rotational accelerations, and rotational velocity, to be measured and calculated [59]. Data from the accelerometers were recorded by a LabVIEW system and post-processed in Matlab and Python 3.8. All of the kinematic data that have been reported and used in this study were filtered using the default 8th-order Butterworth low-pass filter from the “scipy.signal” library of Python. A cutoff frequency of 300 Hz was used to reduce noise in the measured kinematics signals. The 300 Hz frequency was used as this frequency is commonly used by head impact researchers that use similar sensors [62, 63]. Peak kinematics were defined as the maximum value of the resultant trace of the kinematic as an average across the five impact condition repeats.

## Estimates of Regional Peak and Mean MPS using Convolutional Neural Network

Regional peak and mean MPS were predicted using the publicly available pre-trained convolutional neural network (CNN) which can be found at <https://github.com/Jilab-biomechanics/CNN-brain-strains>. The trained CNN developed by Wu et al. (2019) to estimate regional brain strains was selected over other MLHMs in this study as it is publicly available, provides regional brain strain estimations with sufficient accuracy, and was trained on two datasets that included impacts from American football which is a similar sport to rugby [52]. The training dataset also included

**Fig. 1** Drop test conditions for the  $0^\circ$  and  $45^\circ$  impact surfaces used in the study.

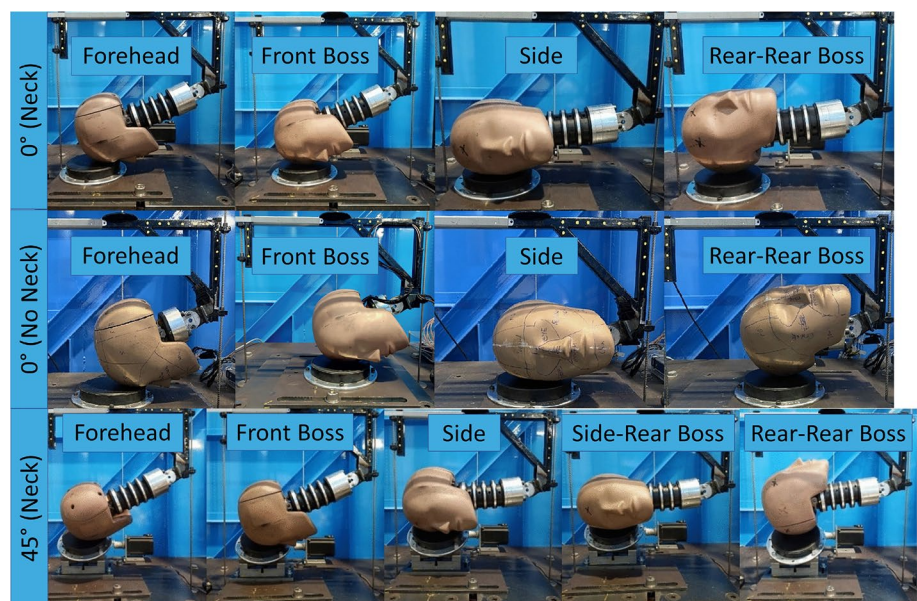


**Table 1** Impact kinematics; Mean (SD)

| Drop heights mm | Impact angle | Impact location          | PLA g              | PRA rad/s <sup>2</sup> | PRV rad/s         | Impact velocity m/s | Impact energy J      |
|-----------------|--------------|--------------------------|--------------------|------------------------|-------------------|---------------------|----------------------|
| 150             | 0°           | Forehead                 | 60.4 (0.2)         | 2790 (25)              | 14.3 (0.1)        | <b>1.69 (0.007)</b> | <b>9.68 (0.003)</b>  |
|                 |              | Front Boss               | 50.1 (0.3)         | 3350 (10)              | 13.4 (0.1)        | 1.65 (0.004)        | 9.31 (0.001)         |
|                 |              | Rear-Rear Boss           | 53 (0.2)           | 3360 (16)              | <b>15.4 (0.3)</b> | 1.66 (0.01)         | 9.33 (0.004)         |
|                 |              | Side                     | 56.1 (0.4)         | 5330 (38)              | 17.7 (0.1)        | 1.64 (0.01)         | 9.15 (0.003)         |
|                 |              | Forehead (No Neck)       | 49.9 (0.5)         | 2380 (89)              | 10.4 (0.3)        | 1.67 (0.01)         | 8.1 (0.004)          |
|                 |              | Front Boss (No Neck)     | 43.2 (0.7)         | 3470 (129)             | 10.5 (0.8)        | 1.65 (0.01)         | 7.91 (0.004)         |
|                 |              | Rear-Rear Boss (No Neck) | 46.8 (0.5)         | 3780 (109)             | 12.1 (0.2)        | 1.68 (0.01)         | 8.19 (0.005)         |
| 150             | 45°          | Side (No Neck)           | <b>67.7 (9.8)</b>  | <b>5600 (251)</b>      | 13 (1.3)          | 1.64 (0.02)         | 7.82 (0.007)         |
|                 |              | Forehead                 | 34.5 (1.1)         | 2660 (135)             | 12.8 (0.5)        | 1.66 (0.03)         | 9.36 (0.01)          |
|                 |              | Front Boss               | 33.2 (0.6)         | 1700 (30)              | 13 (0.1)          | 1.66 (0.02)         | 9.41 (0.006)         |
|                 |              | Rear-Rear Boss           | <b>41.3 (0.2)</b>  | 2040 (27)              | 15.4 (0.09)       | <b>1.73 (0.009)</b> | <b>10.13 (0.003)</b> |
|                 |              | Side                     | 33.5 (1.3)         | <b>4240 (327)</b>      | 17.4 (0.8)        | 1.69 (0.01)         | 9.71 (0.004)         |
| 450             | 0°           | Side-Rear Boss           | 29.7 (1.0)         | 4030 (350)             | <b>19.1 (1.0)</b> | 1.67 (0.02)         | 9.52 (0.007)         |
|                 |              | Forehead                 | 119.6 (0.7)        | 4900 (90)              | 28.5 (0.2)        | 2.89 (0.02)         | <b>28.3 (0.003)</b>  |
|                 |              | Front Boss               | 112.3 (1.3)        | 7830 (276)             | 25.4 (0.1)        | 2.86 (0.01)         | 27.89 (0.002)        |
|                 |              | Rear-Rear Boss           | 115.6 (0.3)        | 8360 (165)             | 28.4 (0.3)        | 2.81 (0.01)         | 26.84 (0.003)        |
|                 |              | Side                     | <b>123.4 (1.9)</b> | <b>12030 (152)</b>     | <b>32.9 (0.4)</b> | 2.75 (0.02)         | 25.74 (0.004)        |
|                 |              | Forehead (No Neck)       | 122.1 (11.0)       | 5290 (455)             | 21.3 (1.5)        | <b>2.93 (0.03)</b>  | 25.34 (0.006)        |
|                 |              | Front Boss (No Neck)     | 102.6 (1.9)        | 7640 (445)             | 21.4 (1.8)        | 2.88 (0.06)         | 24.49 (0.02)         |
| 450             | 45°          | Rear-Rear Boss (No Neck) | 104.5 (2.5)        | 8500 (736)             | 23.3 (1.3)        | 2.92 (0.004)        | 25.13 (0.001)        |
|                 |              | Side (No Neck)           | 110.4 (13.8)       | 10670 (1644)           | 30.7 (0.9)        | 2.4 (0.9)           | 16.96 (0.2)          |
|                 |              | Forehead                 | <b>84.5 (0.3)</b>  | 6230 (60)              | 23.4 (0.14)       | 2.77 (0.02)         | 26.13 (0.003)        |
|                 |              | Front Boss               | 79.4 (1.4)         | 3050 (87)              | 20.5 (0.6)        | <b>2.89 (0.02)</b>  | <b>28.31 (0.005)</b> |
|                 |              | Rear-Rear Boss           | 79.8 (0.6)         | 3830 (174)             | 25.2 (0.2)        | 2.65 (0.02)         | 23.82 (0.005)        |
|                 |              | Side                     | 72.5 (0.3)         | 8260 (155)             | 27.8 (0.4)        | 2.78 (0.02)         | 26.37 (0.004)        |
|                 |              | Side-Rear Boss           | 61.8 (0.2)         | <b>8460 (137)</b>      | <b>31.2 (0.1)</b> | 2.61 (0.02)         | 23.17 (0.005)        |

lab-reconstructed impacts from National Football League which are similar to the drop tests that were used in this study. The CNN was trained on head impacts simulated with the WHIM finite element model of the head. Preprocessing of the head impact time series rotational velocity data was carried out using the preprocessing codes published in the repository, thus ensuring the azimuth and elevation of rotational velocity axes matched that required for the CNN model. The CNN only requires rotational kinematics to estimate the peak and mean MPS values in the brain. This simplification is supported by the finding that linear kinematics have a minimal effect on the peak and distribution of strain throughout the brain [64].

### Statistical Analysis

To assess whether the impact locations, impact angles, the inclusion of a neck, and drop height effect regional peak and mean MPS values, multiple two-way analysis of variance (ANOVA) tests were completed in R using the five data

points from each impact condition. Peak and mean MPS values were analysed to determine the effect of impact location (4 levels), neck inclusion (2 levels), and impact angle (2 levels). Multiple pairwise-comparisons were completed using the post hoc Tukey's Honest Significant Difference (HSD) tests when significance was found. The confidence interval was set to 95% ( $p < 0.05$ ) for the statistical analysis. When comparing the 0° and 45° results, the side-rear boss result was not included to keep the analysis balanced.

## Results

### Head Kinematics

The kinematic measures of each drop test condition are shown in Table 1. The PLAs varied from 33.2 to 122.3 m/s<sup>2</sup>, peak rotational accelerations (PRAs) varied from 1700 to 12030 rad/s<sup>2</sup>, and peak rotational velocities (PRVs) from 10.4 to 32.9 rad/s. For clarity, the maximum values in each



row group of Table 1 have been highlighted in bold. As expected, drop tests from a height of 450 mm resulted in larger peak kinematics. The largest peak rotational velocities for drop tests with an impact angle of 0° occurred during impacts to the side of the head. For drop tests with an impact angle of 45°, the largest PRVs occur as a result of a side-rear boss impact location, followed by impacts to the side.

**Effect of Drop Test Condition on Strain Distribution**

Volume fractions of the rapid estimation FE model within specified MPS ranges are shown in Table 2 for each drop test condition. A large difference was observed in the distribution of MPS between the two drop heights. As expected, condition-matched impacts from 450 mm resulted in a higher proportion of the brain experiencing more severe levels of MPS than those from 150 mm. Notably, volume fractions of the brain greater than 0.1% experiencing MPS greater than 30% were not observed for 150 mm drop tests. At both drop heights, however, impacts to the side of the head resulted in the largest distribution of high MPS, followed by rear-rear

boss, front boss, and finally, forehead, for impacts onto the 0° impact surface (both with and without a neck).

However, this trend was not observed for the 45° tests, as the front boss impact resulted in the largest volume fraction of strain within the 0-10% range for both the 150 mm and 450 mm drop tests. The side impact was the most severe impact location, having the largest volume fraction of strain within the 30-40% range for the 450 mm drop tests and a similar result in the 10-20% range for the 150 mm drop tests.

Figures 2, 3, 4, and 5 present the regional peak and region-averaged MPS for each drop condition and height grouped by test condition (angle and inclusion of neck). These Figures show the maximum MPS values tended to occur in the brainstem for both drop heights, with 92% of the 150 mm impacts and 62% of the 450 mm impacts resulting in maximum peak strain values in this area. In contrast, the cerebellum had the lowest peak MPS values, with 77% of all drop tests resulting in lower peak strains in this region. The peak MPS values ranged from 0.16 to 0.63 for the 450 mm drop tests and 0.09 to 0.34 for the 150 mm drop tests across all drop tests.

**Table 2** Mean (SD) volume fractions of the brain within different strain ranges

| Drop heights mm | Impact angle | Impact location          | Volume fraction of brain between specified strain ranges % |             |             |            |            |
|-----------------|--------------|--------------------------|--|-------------|-------------|------------|------------|
|                 |              |                          | 0–10   | 10–20       | 20–30       | 30–40      | 40–50      |
| 150             | 0°           | Forehead                 | 88.8 (0.11)  | 11.2 (0.11) | –           | –          | –          |
|                 |              | Front Boss               | 77.7 (0.71)  | 22.2 (0.7)  | –           | –          | –          |
|                 |              | Rear-Rear Boss           | 70.5 (0.49)  | 29.5 (0.49) | 0.1 (0.01)  | –          | –          |
|                 |              | Side                     | 67.3 (0.49)  | 32.6 (0.48) | 0.1 (0.01)  | –          | –          |
|                 |              | Forehead (No Neck)       | 95.1 (0.25)  | 4.9 (0.25)  | –           | –          | –          |
|                 |              | Front Boss (No Neck)     | 91.7 (2.44)  | 8.3 (2.44)  | –           | –          | –          |
|                 |              | Rear-Rear Boss (No Neck) | 80.3 (3.87)  | 19.7 (3.86) | –           | –          | –          |
|                 |              | Side (No Neck)           | 71.8 (6.01)  | 28.1 (5.96) | 0.1 (0.04)  | –          | –          |
| 150             | 45°          | Forehead                 | 68.6 (3.68)  | 31.2 (3.48) | 0.2 (0.22)  | –          | –          |
|                 |              | Front Boss               | 79.1 (5.73)  | 20.5 (5.44) | 0.4 (0.29)  | –          | –          |
|                 |              | Rear-Rear Boss           | 81.6 (0.73)  | 18.3 (0.73) | 0 (0.01)    | –          | –          |
|                 |              | Side                     | 51.1 (3.02)  | 45.7 (2.48) | 3.2 (0.59)  | –          | –          |
|                 |              | Side-Rear Boss           | 40.6 (2.8)   | 54.8 (1.65) | 4.5 (1.16)  | –          | –          |
| 450             | 0°           | Forehead                 | 32.9 (0.75)  | 59.4 (0.5)  | 7.5 (0.25)  | 0.2 (0.03) | –          |
|                 |              | Front Boss               | 23.1 (0.18)  | 58.1 (0.87) | 17.5 (0.86) | 1.3 (0.12) | –          |
|                 |              | Rear-Rear Boss           | 14.7 (1.3)   | 65.2 (0.3)  | 18.1 (0.86) | 2 (0.25)   | –          |
|                 |              | Side                     | 6.3 (0.33)   | 64.3 (0.33) | 25.1 (0.33) | 4.1 (0.19) | 0.2 (0)    |
|                 |              | Forehead (No Neck)       | 30.1 (9.34)  | 63.4 (6.85) | 6.2 (2.45)  | 0.2 (0.17) | –          |
|                 |              | Front Boss (No Neck)     | 20.5 (6.39)  | 70.9 (4.77) | 8.5 (2)     | 0.1 (0.01) | –          |
|                 |              | Rear-Rear Boss (No Neck) | 11.6 (2.73)  | 74.6 (0.88) | 13.4 (1.68) | 0.4 (0.2)  | –          |
|                 |              | Side (No Neck)           | 5.5 (2.3)  | 68.1 (5.59) | 23.6 (6.55) | 2.6 (1.28) | 0.1 (0.04) |
| 450             | 45°          | Forehead                 | 20.4 (0.61)  | 58 (0.37)   | 19.1 (0.36) | 2.4 (0.07) | 0 (0.01)   |
|                 |              | Front Boss               | 51.4 (4.08)  | 46.3 (3.25) | 2.3 (0.76)  | –          | –          |
|                 |              | Rear-Rear Boss           | 22.1 (0.49)  | 62.1 (0.28) | 14 (0.29)   | 1.8 (0.12) | –          |
|                 |              | Side                     | 9.4 (0.27)   | 52 (0.59)   | 32.6 (0.43) | 5.7 (0.07) | 0.3 (0.01) |
|                 |              | Side-Rear Boss           | 16.6 (0.59)  | 64.9 (0.93) | 16.2 (1.03) | 2.4 (0.46) | –          |

**Fig. 2** Peak strain for each drop test condition from 150 mm.

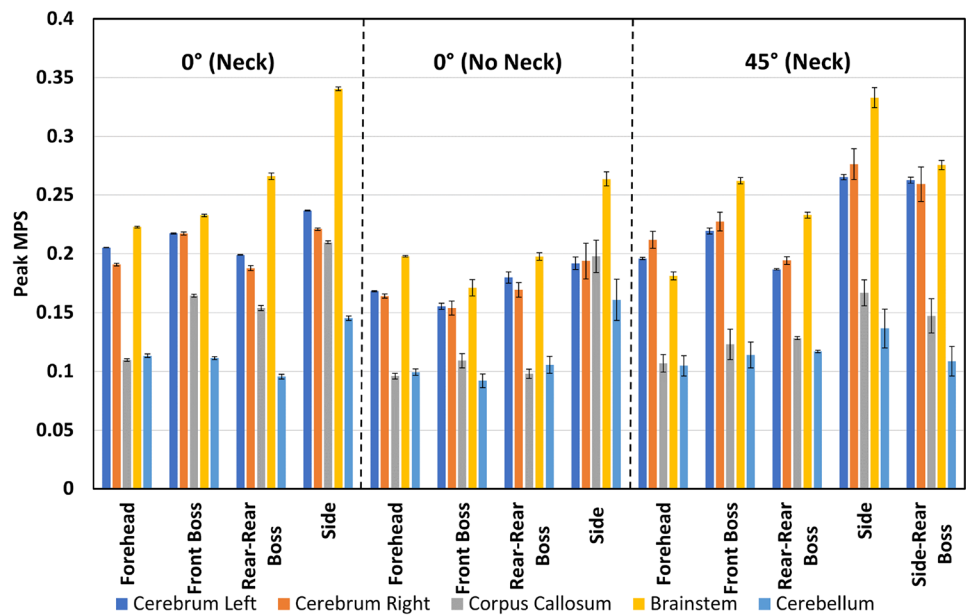
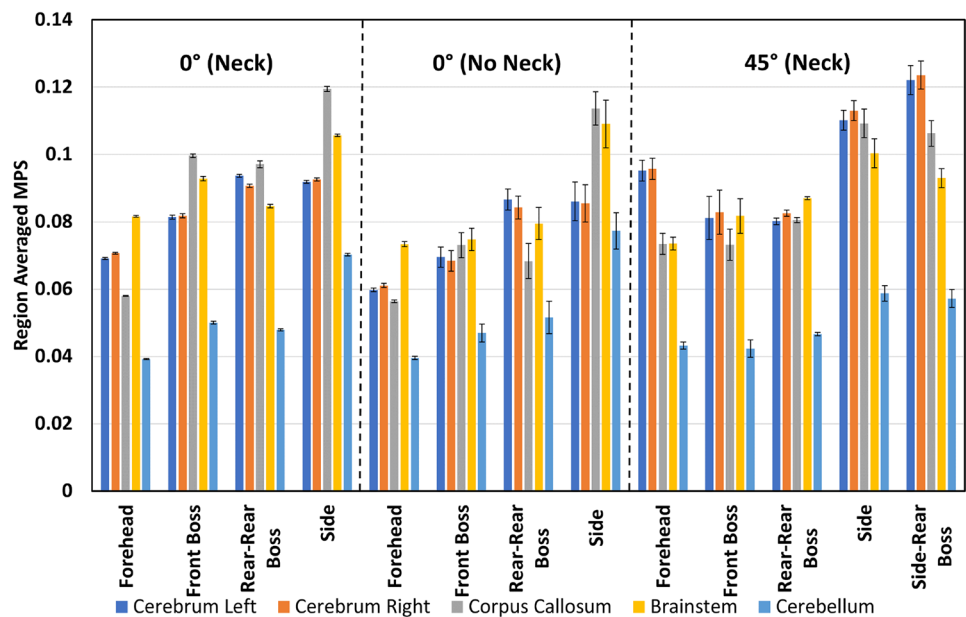


**Fig. 3** Region-averaged MPS for each drop test condition from 150 mm.



Figures 2 and 4 show large differences in regional peak MPS within each drop test condition. Specifically, impacts to the side of the head resulted in the highest peak MPS values for the 0° neck, no neck, and 45° 150 mm drop conditions, with peak MPS of 0.34, 0.26, and 0.33, respectively, all occurring in the brainstem. When interpreted with the volume fraction data in Table 2, it was observed that peak strain occurred in less than 0.1% of the total brain volume. Similarly, the 0° neck and no neck 450 mm drop tests resulted in the highest peak strain values of 0.63 and 0.56, respectively, also occurring in the brainstem. The 45° 450 mm drop test condition resulted in a peak

strain of 0.45, which occurred in the left side of the cerebrum from an impact to the side of the head.

Figures 3 and 5 show the region-averaged values of MPS in each brain region. Although the peak value of MPS is of most interest, the region-averaged MPS in each region offers an indication as to the distribution of MPS values throughout each region. Across 83% of the drop test conditions, the largest region-averaged MPS values occurred as the result of an impact to the side of the head. Region-averaged MPS values varied from 0.04 to 0.26 for the 450 mm drop tests and 0.04 to 0.12 for the 150 mm drop tests.

**Fig. 4** Peak strain for each drop test condition from 450 mm.

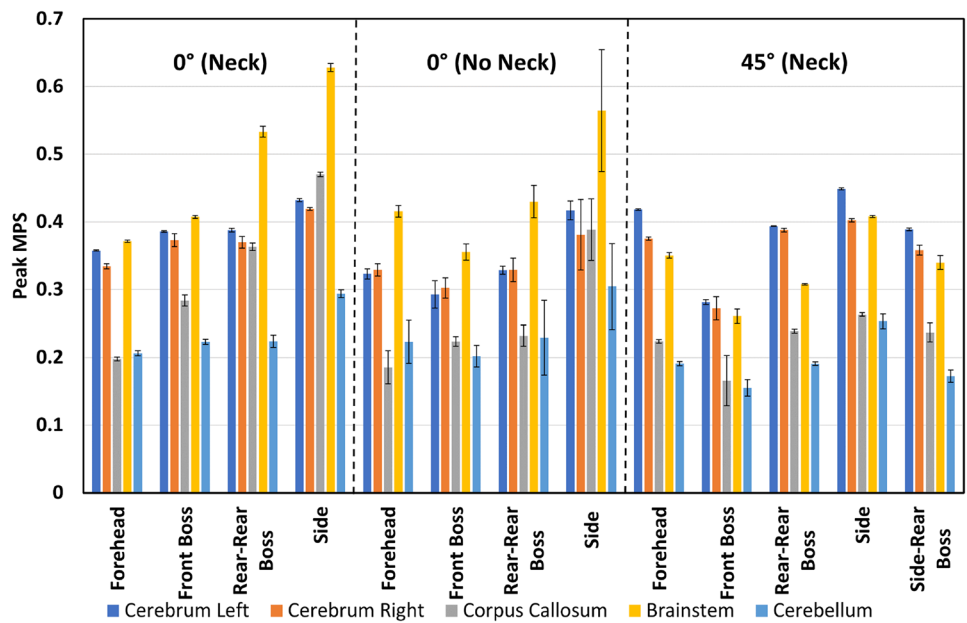
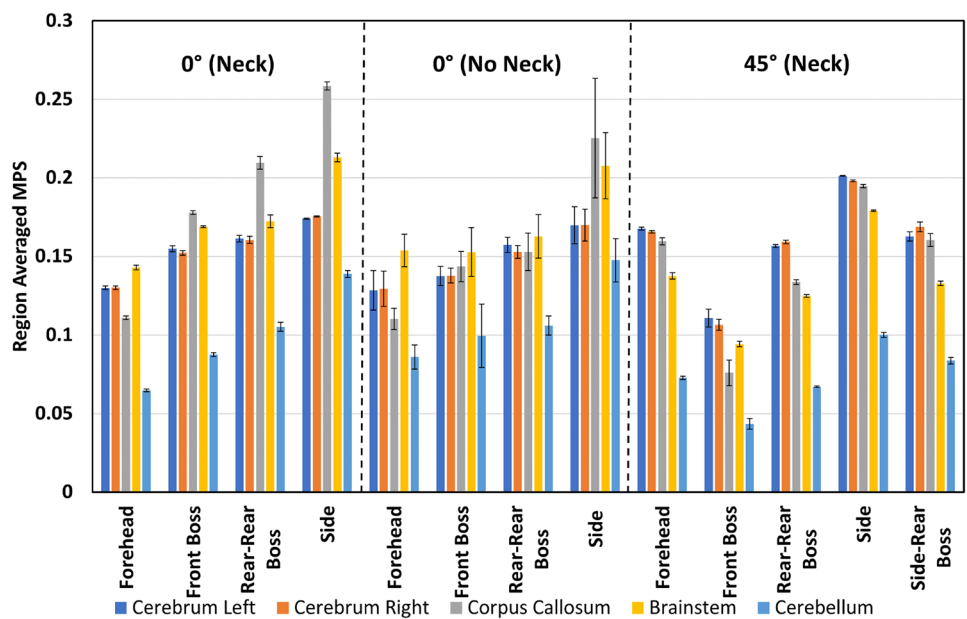


**Fig. 5** Region-averaged MPS for each drop test condition from 450 mm.



**Effect of Impact Location**

Analysis of the 150 mm results revealed that impact location had a significant effect ( $p < 0.05$ ) on the region-averaged and peak MPS values for each region of the brain. However, in almost all of the two-way ANOVA tests that compared the impact location with the impact angle and neck inclusion for the 150 mm drop tests, interaction effects were present. The presence of interaction effects indicates that the relationship between drop test parameters and the resulting MPS metrics is complex.

The analysis of the 150 mm drop tests comparing the effect of impact location and neck inclusion on the region-averaged MPS in the left cerebrum did not show any interaction effect. Impacts to the forehead resulted in the smallest region-averaged MPS in the left side of the cerebrum, followed by front boss impacts. In contrast, impacts to the side of the head and rear-rear boss locations resulted in the largest region-averaged MPS values for both the inclusion and exclusion of the neck. Furthermore, the p-value of 0.79 obtained from the Tukey’s test between the side and rear-rear boss impact location indicated that there was no

significant difference in region-averaged MPS in the left side of the cerebrum caused by these two impact locations.

Analysis of the results of impact location and surface angle for the 150 mm drop height all showed the presence of interaction effects. The interaction effects for the region-averaged MPS were often complex and disordinal due to the variations in trends for different areas of the brain between the impacts where the impact surface was angled at 0° and 45°. The differences between the region-averaged values for drop tests where the impact surface was angled at 0° and 45° were small and ranged from 0 to 0.03. The results showed that forehead impacts resulted in the lowest region-averaged MPS values for impacts where the surface was angled at 0° and 45°, while side impacts resulted in the highest region-averaged MPS values. For the 45° impacts, side impacts resulted in the highest region-averaged MPS values. However, the trends for the other impact locations were inconsistent across different brain regions.

The trends for peak strain values varied across different brain regions. In the left and right cerebrum, the difference between peak strains caused by forehead and front boss was similar, ranging from 0.19 to 0.23. However, side impacts resulted in the highest peak strain values, with 45° impacts leading to significantly higher strain values in the left and right cerebrum (0.27 and 0.28) than 0° impacts (0.24 and 0.22). In contrast, 45° impacts resulted in significantly lower peak strain values in the corpus callosum for front boss, rear-rear boss, and side impacts. No significant difference was observed in peak strain values for 45° and 0° forehead impacts.

The location of impact had a significant effect on the region-averaged and peak MPS values for all 450 mm impacts. Forehead impacts consistently resulted in smaller region-averaged MPS values ranging from 0.065 to 0.15, with front boss and forehead impacts producing the smallest peak strain values. In contrast, side impacts consistently resulted in larger region-averaged and peak MPS values, with peak MPS reaching 0.63 in the brainstem. Results from drop tests where the neck was included typically produced equal or larger peak strain values than identical drop tests that excluded the neck.

The 450 mm drop test results revealed that impact angle and location both have a significant effect on the region-averaged and peak MPS values for all impacts. Similar to the results from the 150 mm drop test, interaction effects were present in the results. The 0° impacts tended to follow the trend of forehead impacts resulting in the lowest region-averaged and peak MPS values, while side impacts resulted in the largest values. Interestingly, for 45° impacts, the front boss impact resulted in the lowest region-averaged and peak MPS values. Across all brain regions, the peak strain values for 450 mm drop tests varied from 0.19 to 0.28. Side impacts consistently produced the highest region-averaged and peak

MPS values compared to other impact locations, with peak strain ranging from 0.25 to 0.45 for 45° side impacts.

### Effect of Surface Angle

The results of the 150 mm drop tests indicate that surface angle had a significant effect on region-averaged MPS values in all regions of the brain, while only showing significant differences in peak strain values in the right side of the cerebrum, corpus callosum, and brainstem. Tukey's tests demonstrated that the 45° impact surface resulted in higher region-averaged MPS values in the left and right side of the cerebrum, and lower region-averaged MPS values in the corpus callosum, brainstem, and cerebellum. Additionally, the 45° impact surface led to larger peak strain values in the right side of the cerebrum and lower peak strain values in the corpus callosum and brainstem.

Similarly, the 450 mm drop tests also demonstrated significant effects of surface angle on region-averaged and peak MPS values in all regions of the brain except for the left side of the cerebrum. The results of Tukey's tests for the 450 mm drop tests follow the same trends as the 150 mm drop tests, with the 45° impact surface leading to higher region-averaged MPS values in the left and right side of the cerebrum, and lower region-averaged MPS values in the cerebrum, corpus callosum, and brainstem. Moreover, the peak strain values were smaller when a 45° impact surface was used. These findings suggest that surface angle should be taken into account when designing and evaluating protective measures for brain injury.

### Effect of Neck Inclusion

Analysis of the 150 mm results revealed that the inclusion of the neck had a significant effect on the region-averaged and peak MPS values for all areas of the brain except for the peak strain in the cerebellum. The results from the post hoc Tukey's test show that the inclusion of the neck results in higher region-averaged MPS values for all brain regions except for the cerebellum. The trends for the peak strain values follow the same trends, with all regions having higher peak strain values with the inclusion of the neck except for the peak strain in the cerebellum where there was no significant difference between the inclusion and exclusion of the neck.

Analysis of the 450 mm results showed that the inclusion of the neck had a significant effect on the region-averaged and peak MPS for all impacts except the region-averaged MPS in the brainstem and peak strain in the cerebellum. In particular, the inclusion of the neck resulted in lower region-averaged MPS values for the cerebellum but higher region-averaged and peak MPS values for all other regions. The largest difference in peak strain values occurred in the



corpus callosum, where a rear-rear boss impact resulted in a peak strain of 0.23 when the neck was not included, and 0.36 when the neck was included. The differences between the neck and no-neck peak strains were larger than the region-averaged MPS values.

## Discussion

The focus of this study was to investigate the effects that drop test parameters have on regional peak and mean MPS location and severity. To complete this, five impact locations were tested at two impact angles, two drop heights and both including and excluding the neck. To generate the results in this study, the velocity profiles obtained from the controlled lab impacts were input into a pre-trained CNN model [52] to rapidly estimate regional peak and mean MPS values. The resulting regional peak and mean MPS values found that the drop test parameters of the impact location, impact angle, and the inclusion of the neck all had a significant result on the mean and peak regional MPS values. However, interaction effects were often present when analysing the pairs of drop test parameters, indicating that the relationship between drop test parameters and the resulting regional peak and mean MPS is complex.

### Effect of Drop Height

When looking at the effect of increasing drop height on strain values across all regions of the brain, the results showed that an increase in drop height led to significantly higher impact energy as shown Table 1. As the impact energy increases, the head experiences larger forces and accelerations, leading to greater deformation of brain tissue and higher strain values. This relationship between impact energy and brain strain has been documented previously [39]. However, when excluding side-rear boss impacts, impacts to the side of the head consistently resulted in the larger regional peak and mean MPS values. These results show that impact energy alone does not directly determine the resulting regional peak and mean MPS, thus indicating a more complex interaction between variables. This highlights that factors such as impact location and impact compliance (the overall stiffness of an impact) play a critical role in the resulting head kinematics [39, 58, 61] and thus brain injury. Interestingly, the trends between impact location and resulting strain were not always consistent between the 150 mm and 450 mm drop heights used in this study.

### Effect of Impact Surface Angle

When considering the head kinematics in Table 1, the results showed that the 450 mm drop tests resulted in the highest

peak kinematics. Impact location and angle significantly influenced peak rotational velocity, with the largest peak rotational velocity of 32.9 rad/s for drop tests with an impact angle of 0° occurring as a result of an impact to the side of the head, and for drop tests with an impact angle of 45°, the peak rotational velocities of 31.2 rad/s occurred as a result of a side-rear boss impact location.

The difference in rotational velocities and regional peak and mean MPS from side-rear boss and side impacts compared to frontal impacts can be attributed to the oblique nature of the force vector during the collision. As the impact force is not applied in line with the centre of mass of the brain, a rotational moment is applied to the brain. This rotational moment induces internal shear forces and shear-induced tissue damage [14]. There is considerable literature that discusses the rotational kinematics of the head as a main mechanism for TBI [65–68]. The results from the drop tests in this paper corroborate with these studies in terms of predicted MPS. The results of this paper also highlight the complex interactions between each of the laboratory drop test parameters.

### Effect of Neck Inclusion

Overall, the inclusion of the neck in the drop test results had a significant effect on the region-averaged and peak MPS values for all areas of the brain except for the peak strain in the cerebellum. In both the 150 mm and 450 mm drop tests, the inclusion of the neck resulted in higher region-averaged and peak MPS values for most regions of the brain. However, the inclusion of the neck resulted in lower region-averaged MPS values for the cerebellum in the 450 mm drop tests.

The additional mass of the neck is unlikely to be the reason for higher strain levels when the neck is included. As mass is added to the impacting body, the peak kinematics generally decrease. The inclusion of the neck extended the duration of the rotational velocity peak (i.e. the duration and shape of the rotational acceleration was affected, but not the peak). No measurable effect on the linear acceleration was observed. This result conforms with previous work that has investigated how neck inclusion impacts the kinematics of the headform. Sitt et al. [58] have shown that inclusion of the neck during drop testing did not significantly influence the peak linear and rotational accelerations, or the peak rotational velocity for both height- and energy-matched impacts. It did, however, significantly influence the shape of the rotational velocity kinematic trace and, by extension, the rotational acceleration trace. Inclusion of the neck during drop testing extended the duration of the rotational velocity, especially in the side impact location, where the occipital condyle joint of the HIII head restricts rotational motion in the direction of the impact force. This extension of the

duration of the rotational velocity peak likely explains the higher MPS values seen between impact with and without the neck. In addition, muscle activation of the neck has been shown to reduce the severity of TBI [69]. Such factors could provide a basis future work that could look to incorporate when investigating brain strains and TBI in rugby.

### Comparisons with Previous Studies

There are several studies that have investigated peak MPS values using simulations based on measured head kinematics [39, 70, 71]. Typical peak MPS values from these studies have ranged from 0.1 to 0.55. The results from this study are within a similar range, with peak strain values ranging from 0.09 to 0.63. The results from this study showed that impact location significantly altered the resulting kinematics and, by extension, peak and mean regional MPS values. In agreement with previous literature [39–41], impacts to the side of the head resulted in significantly higher regional MPS compared to forehead impacts.

### Limitations and Future Work

The current study presents a novel approach to investigating the effects of various drop test parameters on regional peak and mean MPS using lab-controlled impacts. However, several limitations should be noted. Firstly, the accuracy of the CNN MLHM to make regional MPS predictions is one limitation of the study. As the CNN model was trained on some datasets that included boxing, and mixed martial arts impacts, this is source of inaccuracy for the resulting MPS predictions. The CNN was used as it provides novel insights into what the resulting brain strain distribution may look like for the different drop test conditions. This CNN MLHM was used as it provides far greater insights than head impact kinematics or head injury criteria alone. However, care should be taken when trying to extrapolate the results from this model to actual brain injuries in sport, as these are unlikely to be exactly the same as what would develop in the brain. The focus of this study was not to see a human head responds, instead the focus was to investigate differences in regional MPS predictions with a range of laboratory drop test conditions. The MPS prediction is an additional metric that provides a close insight to injury. Secondly, the use of the HIII headform results in some limitations, as different headform shapes and sizes have been found to result in significantly different PRAs and PRVs [72, 73]. As the HIII headform is likely to have a different response to a real human head, it is difficult to correlate the drop test responses to that of a human head. As the CNN model uses the rotational velocity profile as an input, the use of a headform will result in different strain predictions to that of a human head. Although these predictions might not be exactly the same as what we

would expect in a human head, the trends and regional strain predictions provide insight into what we might expect to see. The headform used in this study does not account for individual differences in brain tissue properties, which may also affect the accuracy of the results. Previous work has shown that brain size has a significant impact on injury susceptibility, with larger brains tending to have a higher risk of injury [74]. However, the relationship between brain size and injury risk is not always strictly linear, as other factors can also play a role. Thirdly, the study only investigated a limited range of drop test parameters including impact location and angle, drop height, and the inclusion of a neck. Other important factors, such as differences in loading rate due to the compliance of the impact surfaces, were not investigated. Weight differences were also not included as a parameter for this study, a study by Gimble and Hoshizaki found that the PLA decreased when head mass was increased for the same impact velocity [75]. Lastly, it is worth noting that the use of lab-controlled drop tests may not fully reflect the complexity and variability of real-world head impacts. While lab-controlled experiments allow for the systematic investigation of different parameters, they may not fully capture the randomness and variability of on-field impacts. By considering the impact conditions and injury mechanisms specific to TBIs in rugby, future work could investigate a wider range of impact parameters to identify the specific variables that cause increases in predicted brain strains. Knowledge of these variables will be used to guide helmet innovations and improve the quality of helmet protection to reduce the resulting brain strains incurred from playing rugby. The approach of using a CNN to predict regional peak and mean MPS brain strain values provides an additional metric for developing protective equipment such as headgear in rugby. The brain strain values also enable comparisons between different injury prevention methods, such as helmets, to be evaluated in terms of brain strain rather than other brain injury criteria which do not give a region-specific assessment of injury.

**Acknowledgments** We would like to thank Songbai Ji for his help in the use of the rapid estimation FE model.

**Funding** Open Access funding enabled and organized by CAUL and its Member Institutions.

**Open Access** This article is licensed under a Creative Commons Attribution 4.0 International License, which permits use, sharing, adaptation, distribution and reproduction in any medium or format, as long as you give appropriate credit to the original author(s) and the source, provide a link to the Creative Commons licence, and indicate if changes were made. The images or other third party material in this article are included in the article's Creative Commons licence, unless indicated otherwise in a credit line to the material. If material is not included in the article's Creative Commons licence and your intended use is not permitted by statutory regulation or exceeds the permitted use, you will

need to obtain permission directly from the copyright holder. To view a copy of this licence, visit <http://creativecommons.org/licenses/by/4.0/>.

## References

- Centers for Disease Control: Cdc's report to congress on traumatic brain injury epidemiology and rehabilitation. Washington, D. C: CDC (2016)
- Marr, A.L., Coronado, V.G.: Central nervous system injury surveillance data submission standards—2002. Atlanta, GA: US Department of Health and Human Services, CDC (2004)
- Draper, N., Kabaliuk, N., Stitt, D., Alexander, K.: Potential of soft-shelled rugby headgear to reduce linear impact accelerations. *Journal of Healthcare Engineering* **2021** (2021)
- Kimpara, H., and M. Iwamoto. Mild traumatic brain injury predictors based on angular accelerations during impacts. *Annals of Biomedical Engineering*. 40(1):114–126, 2012.
- Young, T.J.: Predicting mild traumatic brain injury with injury risk functions. (2013). Brain Injuries and Biomechanics Symposium
- Rowson, S., S. M. Duma, J. G. Beckwith, J. J. Chu, R. M. Greenwald, J. J. Crisco, P. G. Brolinson, A.-C. Duhaime, T. W. McAllister, and A. C. Maerlender. Rotational head kinematics in football impacts: an injury risk function for concussion. *Annals of Biomedical Engineering*. 40(1):1–13, 2012.
- King, D., P. A. Hume, M. BrugHELLI, and C. Gissane. Instrumented mouthguard acceleration analyses for head impacts in amateur rugby union players over a season of matches. *The American Journal of Sports Medicine*. 43(3):614–624, 2015.
- King, D., P. Hume, C. Gissane, and T. Clark. Measurement of head impacts in a senior amateur rugby league team with an instrumented patch: exploratory analysis. *ARC Journal of Research in Sports Medicine*. 2(1):9–20, 2017.
- King, D. A., P. A. Hume, C. Gissane, D. C. Kieser, and T. N. Clark. Head impact exposure from match participation in women's rugby league over one season of domestic competition. *Journal of Science and Medicine in Sport*. 21(2):139–146, 2018.
- King, D. A., P. A. Hume, C. Gissane, and T. N. Clark. Similar head impact acceleration measured using instrumented ear patches in a junior rugby union team during matches in comparison with other sports. *Journal of Neurosurgery: Pediatrics*. 18(1):65–72, 2016.
- Marshall, S. W., and R. J. Spencer. Concussion in rugby: the hidden epidemic. *Journal of Athletic Training*. 36(3):334, 2001.
- Hendricks, S., E. Jordaan, and M. Lambert. Attitude and behaviour of junior rugby union players towards tackling during training and match play. *Safety Science*. 50(2):266–284, 2012.
- Gardner, A. J., G. L. Iverson, W. H. Williams, S. Baker, and P. Stanwell. A systematic review and meta-analysis of concussion in rugby union. *Sports Medicine*. 44(12):1717–1731, 2014.
- Meaney, D. F., and D. H. Smith. Biomechanics of concussion. *Clinics in Sports Medicine*. 30(1):19–31, 2011.
- Zhan, X., Y. Li, Y. Liu, A. G. Domel, H. V. Alizadeh, S. J. Raymond, J. Ruan, S. Barbat, S. Tiernan, O. Gevaert, et al. The relationship between brain injury criteria and brain strain across different types of head impacts can be different. *Journal of the Royal Society Interface*. 18(179):20210260, 2021.
- Vynorius, K. C., A. M. Paquin, and D. R. Seichepine. Lifetime multiple mild traumatic brain injuries are associated with cognitive and mood symptoms in young healthy college students. *Frontiers in Neurology*. 7:188, 2016.
- Meaney, D. F., and D. H. Smith. Biomechanics of concussion. *Clin Sports Med*. 30(1):19–31, 2011. <https://doi.org/10.1016/j.csm.2010.08.009.1556-228x>.
- Guskiewicz, K. M., S. W. Marshall, J. Bailes, M. McCrea, R. C. Cantu, C. Randolph, and B. D. Jordan. Association between recurrent concussion and late-life cognitive impairment in retired professional football players. *Neurosurgery*. 57(4):719–2671926, 2005. <https://doi.org/10.1093/neurosurgery/57.4.719.1524-4040>.
- McMillan, T., P. McSkimming, J. Wainman-Lefley, L. Maclean, J. Hay, A. McConnachie, and W. Stewart. Long-term health outcomes after exposure to repeated concussion in elite level: rugby union players. *Journal of Neurology, Neurosurgery & Psychiatry*. 88(6):505–511, 2017.
- Grinberg, L. T., R. Anghinah, C. F. Nascimento, E. Amaro, R. P. Leite, M. G. M. Martin, M. S. Naslavsky, L. T. Takada, W. J. Filho, C. A. Pasqualucci, and R. Nitri. Chronic traumatic encephalopathy presenting as Alzheimer's disease in a retired soccer player. *Journal of Alzheimer's disease*. 54(1):169–174, 2016.
- Sharp, D. J., and P. O. Jenkins. Concussion is confusing us all. *Practical Neurology*. 15(3):172, 2015.
- Gardner, A., G. L. Iverson, C. R. Levi, P. W. Schofield, F. Kay-Lambkin, R. M. Kohler, and P. Stanwell. A systematic review of concussion in rugby league. *British journal of sports medicine*. 49(8):495–498, 2015.
- Hinton-Bayre, A., G. Geffen, and P. Friis. Presentation and mechanisms of concussion in professional rugby league football. *Journal of Science and Medicine in Sport*. 7(3):400–404, 2004. [https://doi.org/10.1016/S1440-2440\(04\)80035-5](https://doi.org/10.1016/S1440-2440(04)80035-5).
- Hoshizaki, T., A. M. Post, C. E. Zepa, E. Legace, T. B. Hoshizaki, and M. D. Gilchrist. Evaluation of two rotational helmet technologies to decrease peak rotational acceleration in cycling helmets. *Scientific Reports*. 12(1):1–8, 2022.
- Takhounts, E.G., Craig, M.J., Moorhouse, K., McFadden, J., Hasija, V.: Development of brain injury criteria (bric). *Stapp Car Crash J* **57**, 243–66 (2013)
- Rowson, S., and S. M. Duma. Brain injury prediction: assessing the combined probability of concussion using linear and rotational head acceleration. *Annals of Biomedical Engineering*. 41(5):873–882, 2013.
- Ji, S., and W. Zhao. A pre-computed brain response atlas for instantaneous strain estimation in contact sports. *Annals of Biomedical Engineering*. 43(8):1877–1895, 2015.
- King, A.I., Yang, K.H., Zhang, L., Hardy, W., Viano, D.C.: Is head injury caused by linear or angular acceleration. In: IRC-OBI Conference, vol. 12 (2003). Lisbon, Portugal
- Ji, S., W. Zhao, Z. Li, and T. W. McAllister. Head impact accelerations for brain strain-related responses in contact sports: a model-based investigation. *Biomechanics and Modeling in Mechanobiology*. 13(5):1121–1136, 2014.
- Levy, Y., K. Bian, L. Patterson, R. Ouckama, and H. Mao. Head kinematics and injury metrics for laboratory hockey-relevant head impact experiments. *Annals of Biomedical Engineering*. 49(10):2914–2923, 2021.
- Holbourn, A. Mechanics of head injuries. *The Lancet*. 242(6267):438–441, 1943.
- Gennarelli, T. A., L. E. Thibault, and D. I. Graham. Diffuse axonal injury: an important form of traumatic brain damage. *The Neuroscientist*. 4(3):202–215, 1998.
- Gabler, L. F., J. R. Crandall, and M. B. Panzer. Development of a second-order system for rapid estimation of maximum brain strain. *Ann Biomed Eng*. 47(9):1971–1981, 2019. <https://doi.org/10.1007/s10439-018-02179-9>.
- Gabler, L. F., H. Joodaki, J. R. Crandall, and M. B. Panzer. Development of a single-degree-of-freedom mechanical model for predicting strain-based brain injury responses. *Journal of Biomechanical Engineering*. 140(3):031002, 2018.

35. Giudice, J. S., W. Zeng, T. Wu, A. Alshareef, D. F. Shedd, and M. B. Panzer. An analytical review of the numerical methods used for finite element modeling of traumatic brain injury. *Annals of Biomedical Engineering*. 47(9):1855–1872, 2019.
36. Hernandez, F., L. C. Wu, M. C. Yip, K. Laksari, A. R. Hoffman, J. R. Lopez, G. A. Grant, S. Kleiven, and D. B. Camarillo. Six degree-of-freedom measurements of human mild traumatic brain injury. *Ann Biomed Eng*. 43(8):1918–1934, 2015. <https://doi.org/10.1007/s10439-014-1212-4>.
37. Sahoo, D., C. Deck, and R. Willinger. Development and validation of an advanced anisotropic visco-hyperelastic human brain Fe model. *Journal of the Mechanical Behavior of Biomedical Materials*. 33:24–42, 2014.
38. Li, X., Z. Zhou, and S. Kleiven. An anatomically detailed and personalizable head injury model: Significance of brain and white matter tract morphological variability on strain. *Biomechanics and Modeling in Mechanobiology*. 20(2):403–431, 2021.
39. Elkin, B. S., L. F. Gabler, M. B. Panzer, and G. P. Siegmund. Brain tissue strains vary with head impact location: a possible explanation for increased concussion risk in struck versus striking football players. *Clinical Biomechanics*. 64:49–57, 2019.
40. Milef, G.M., Müller, L.E., DiGuglielmo, D.M., Payne, T.D., Filben, T.M., Urban, J.E., Stitzel, J.D.: Head impact kinematics and brain deformation in paired opposing youth football players. *Journal of Applied Biomechanics* 1(aop), 1–12 (2022)
41. Zhang, L., K. H. Yang, and A. I. King. Comparison of brain responses between frontal and lateral impacts by finite element modeling. *Journal of Neurotrauma*. 18(1):21–30, 2001.
42. Miller, L. E., J. E. Urban, and J. D. Stitzel. Development and validation of an atlas-based finite element brain model. *Biomechanics and Modeling in Mechanobiology*. 15(5):1201–1214, 2016.
43. Zhao, W., and S. Ji. Mesh convergence behavior and the effect of element integration of a human head injury model. *Annals of biomedical engineering*. 47(2):475–486, 2019.
44. Mao, H., L. Zhang, B. Jiang, V. V. Genthikatti, X. Jin, F. Zhu, R. Makwana, A. Gill, G. Jandir, A. Singh, et al. Development of a finite element human head model partially validated with thirty five experimental cases. *Journal of biomechanical engineering*. 135(11):111002, 2013.
45. Ghazi, K., S. Wu, W. Zhao, and S. Ji. Instantaneous whole-brain strain estimation in dynamic head impact. *Journal of Neurotrauma*. 38(8):1023–1035, 2021.
46. Liu, Y., A. G. Domel, N. J. Cecchi, E. Rice, A. A. Callan, S. J. Raymond, Z. Zhou, X. Zhan, Y. Li, M. M. Zeineh, et al. Time window of head impact kinematics measurement for calculation of brain strain and strain rate in American football. *Annals of biomedical engineering*. 49(10):2791–2804, 2021.
47. Gabler, L. F., J. R. Crandall, and M. B. Panzer. Development of a metric for predicting brain strain responses using head kinematics. *Annals of biomedical engineering*. 46(7):972–985, 2018.
48. Zhan, X., Liu, Y., Cecchi, N.J., Gevaert, O., Zeineh, M.M., Grant, G.A., Camarillo, D.B.: Rapidly and accurately estimating brain strain and strain rate across head impact types with transfer learning and data fusion. arXiv preprint [arXiv:2108.13577](https://arxiv.org/abs/2108.13577) (2021)
49. Zhao, W., C. Kuo, L. Wu, D. B. Camarillo, and S. Ji. Performance evaluation of a pre-computed brain response atlas in dummy head impacts. *Annals of biomedical engineering*. 45(10):2437–2450, 2017.
50. Ji, S., W. Zhao, J. C. Ford, J. G. Beckwith, R. P. Bolander, R. M. Greenwald, L. A. Flashman, K. D. Paulsen, and T. W. McAllister. Group-wise evaluation and comparison of white matter fiber strain and maximum principal strain in sports-related concussion. *Journal of neurotrauma*. 32(7):441–454, 2015.
51. Zhao, W., and S. Ji. White matter anisotropy for impact simulation and response sampling in traumatic brain injury. *Journal of neurotrauma*. 36(2):250–263, 2019.
52. Wu, S., W. Zhao, K. Ghazi, and S. Ji. Convolutional neural network for efficient estimation of regional brain strains. *Scientific Reports*. 9(1):17326, 2019. <https://doi.org/10.1038/s41598-019-53551-1>.
53. Deck, C., N. Bourdet, A. Trog, F. Meyer, V. Noblet, and R. Willinger. Deep learning method to assess brain injury risk. *International Journal of Crashworthiness*. 28(6):760–769, 2023. <https://doi.org/10.1080/13588265.2022.2130600>.
54. Zhan, X., Y. Liu, S. J. Raymond, H. V. Alizadeh, A. G. Domel, O. Gevaert, M. M. Zeineh, G. A. Grant, and D. B. Camarillo. Rapid estimation of entire brain strain using deep learning models. *IEEE Transactions on Biomedical Engineering*. 68(11):3424–3434, 2021.
55. Tamai, S., Miyazaki, Y., Yamamoto, H., Yoshii, K., Amamori, I.: Construction of a prediction model for the time series of brain strain of a novel head surrogate using deep learning. In: 27th International Technical Conference on the Enhanced Safety of Vehicles (ESV) National Highway Traffic Safety Administration (2023)
56. Zhan, X., Liu, Y., Cecchi, N.J., Gevaert, O., Zeineh, M.M., Grant, G.A., Camarillo, D.B.: Brain deformation estimation with transfer learning for head impact datasets across impact types. *IEEE Transactions on Biomedical Engineering*, 1–12 (2024) <https://doi.org/10.1109/TBME.2024.3354192>
57. Zhan, X., Sun, J., Liu, Y., Cecchi, N.J., Le Flao, E., Gevaert, O., Zeineh, M.M., Camarillo, D.B.: Adaptive machine learning head model across different head impact types using unsupervised domain adaptation and generative adversarial networks. *IEEE Sensors Journal*, 1–1 (2024) <https://doi.org/10.1109/JSEN.2023.3349213>
58. Stitt, D., N. Kabaliuk, K. Alexander, and N. Draper. Drop test kinematics using varied impact surfaces and head/neck configurations for rugby headgear testing. *Annals of Biomedical Engineering*. 50(11):1633–1647, 2022. <https://doi.org/10.1007/s10439-022-03045-5>.
59. Padgaonkar, A. J., K. W. Krieger, and A. I. King. Measurement of angular acceleration of a rigid body using linear accelerometers. *Journal of Applied Mechanics*. 42(3):552–556, 1975. <https://doi.org/10.1115/1.3423640>.
60. Draper, N., Kabaliuk, N., Stitt, D., Alexander, K.: Research article potential of soft-shelled rugby headgear to reduce linear impact accelerations. *Journal of Healthcare Engineering* (2021)
61. Stitt, D., Kabaliuk, N., Alexander, K., Draper, N.: Potential of soft-shell rugby headgear to mitigate linear and rotational peak accelerations. *Annals of Biomedical Engineering*, 1–19 (2022)
62. Cecchi, N.J., Callan, A.A., Watson, L.P., Liu, Y., Zhan, X., Vegesna, R.V., Pang, C., Le Flao, E., Grant, G.A., Zeineh, M.M., et al.: Padded helmet shell covers in American football: a comprehensive laboratory evaluation with preliminary on-field findings. *Annals of biomedical engineering*, 1–14 (2023)
63. Field, B., Waddington, G., McKune, A., Goecke, R., Gardner, A.J.: Validation of an instrumented mouthguard in rugby union—a pilot study comparing impact sensor technology to video analysis. *Frontiers in Sports and Active Living* 5 (2023)
64. Liu, Y., Zhan, X., Domel, A.G., Fanton, M., Zhou, Z., Raymond, S.J., Alizadeh, H.V., Cecchi, N.J., Zeineh, M., Grant, G.: Theoretical and numerical analysis for angular acceleration being determinant of brain strain in mtbi. arXiv preprint [arXiv:2012.13507](https://arxiv.org/abs/2012.13507) (2020)
65. Gennarelli, T., Adams, J., Graham, D.: Acceleration induced head injury in the monkey. i. the model, its mechanical and physiological correlates. In: *Experimental and Clinical*



- Neuropathology: Proceedings of the First European Neuropathology Meeting, Vienna, May 6–8, 1980, pp. 23–25 (1981). Springer
66. Kleiven, S.: Predictors for traumatic brain injuries evaluated through accident reconstructions. Technical report, SAE Technical Paper (2007)
  67. Takhounts, E. G., S. A. Ridella, V. Hasija, R. E. Tannous, J. Q. Campbell, D. Malone, K. Danelson, J. Stitzel, S. Rowson, and S. Duma. Investigation of traumatic brain injuries using the next generation of simulated injury monitor (simon) finite element head model. *Stapp car crash journal*. 52:1, 2008.
  68. Weaver, A. A., K. A. Danelson, and J. D. Stitzel. Modeling brain injury response for rotational velocities of varying directions and magnitudes. *Annals of biomedical engineering*. 40:2005–2018, 2012.
  69. Jin, X., Feng, Z., Mika, V., Li, H., Viano, D.C., Yang, K.H.: The role of neck muscle activities on the risk of mild traumatic brain injury in American football. *Journal of biomechanical engineering* **139**(10) (2017)
  70. Michio Clark, J., Post, A., Blaine Hoshizaki, T., Gilchrist, M.D.: Distribution of brain strain in the cerebrum for laboratory impacts to ice hockey goaltender masks. *Journal of Biomechanical Engineering* **140**(12) (2018)
  71. Zhang, L., K. H. Yang, and A. I. King. A proposed injury threshold for mild traumatic brain injury. *J. Biomech. Eng.* 126(2):226–236, 2004.
  72. Bland, M.L., McNally, C., Rowson, S.: Headform and neck effects on dynamic response in bicycle helmet oblique impact testing. In: Proceedings of the IRCOBI Conference. Athens, Greece, pp. 413–423 (2018)
  73. Oeur, R. A., M. D. Gilchrist, and T. B. Hoshizaki. Interaction of impact parameters for simulated falls in sport using three different sized hybrid iii headforms. *International journal of crashworthiness*. 24(3):326–335, 2019.
  74. Wu, T., J. A. Rifkin, A. C. Rayfield, E. D. Anderson, M. B. Panzer, and D. F. Meaney. Concussion prone scenarios: a multi-dimensional exploration in impact directions, brain morphology, and network architectures using computational models. *Annals of biomedical engineering*. 50(11):1423–1436, 2022.
  75. Gimbel, G. M., and T. B. Hoshizaki. Compressive properties of helmet materials subjected to dynamic impact loading of various energies. *European Journal of Sport Science*. 8(6):341–349, 2008.

**Publisher's Note** Springer Nature remains neutral with regard to jurisdictional claims in published maps and institutional affiliations.